Analysis of multiple alleles reveals the roles of *dpy-19* in *C. elegans* neuroblast migration

Senior Thesis

Presented to

The Faculty of the Department of Molecular Biology

Colorado College

In Addition of the Requirements for the Degree
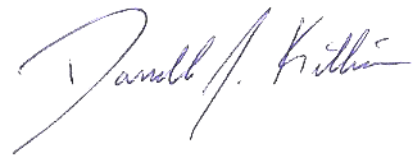
Bachelor of Arts

By

Ana Grace Musto

May 2022

Honor Code Signature: *Ana Musto*

Primary Thesis Advisor

Darrell J. Killian, Ph.D.

Second Thesis Reader

Matt Bowers, Ph.D.

ABSTRACT

A key component of nervous system development is the migration of undifferentiated cells, termed neuroblasts, and their differentiation into neurons upon arrival at a target location. Mutations affecting the mechanisms responsible for neuroblast migration and localization can lead to numerous developmental defects. In humans, abnormal neuroblast migration results in structurally abnormal or missing areas of the brain in the cerebral hemispheres, cerebellum, brainstem, or hippocampus. Recently, we isolated a mutant strain of *Caenorhabditis elegans* exhibiting a Dumpy phenotype (short body length) and with aberrant localization of neurons that are derived from a neuroblast lineage known as the Q lineage. The mutation was renamed *dpy-19(cnj1)* once sequencing revealed that the mutation is a 12,495 bp deletion/12bp insertion affecting the *dpy-19* gene. *dpy-19* encodes a *C*-mannosyltransferase that glycosylates the tryptophan residues in thrombospondin repeats of cell surface receptors. While not all substrates of DPY-19 are known, one target is MIG-21, which requires glycosylation before its soluble form can be secreted during Q lineage migration. Previous studies have implicated *dpy-19* in the initial polarization of Q neuroblasts (QL and QR) and in the direction of their migrations, however, these early studies were not performed using a true null allele of *dpy-19* and did not have the benefit of fluorescent markers for live cell imaging. This motivated us to analyze the true null phenotype of *dpy-19*. While the *dpy-19(cnj1)* allele we isolated is predicted to completely remove *dpy-19* function, it also results in a deletion of other genes. To eliminate the possibility that these other genes impact the phenotype, a true null allele, *dpy-19(cnj5)* was developed using CRISPR to study the neuronal and body length defects in detail. Firstly, we conducted a body length analysis comparing all available *dpy-19* mutant strains to controls to determine the role of *dpy-19* in animal length. Secondly, we scored the same mutants using GFP as a marker for Q-lineage neurons to

determine how the loss of *dpy-19* affects neuron positioning and migration. Lastly, we visualized QR and QL cells in L1 stage animals marked with GFP and screened for the direction of pseudopod growth to assess the impact of the loss of *dpy-19* on the initial polarization of the neuroblasts. Our study confirms past studies, and also suggests that *dpy-19* is important for the migration of the entire Q cell lineage. Four homologs of DPY-19 exist in humans, DPY19L1-4, suggesting conserved molecular function. DPY19L1 and DPY19L3 are also *C*-mannosyltransferases and are involved in radial migration of glutamatergic neurons in the developing cerebral cortex, and sperm head elongation and acrosome formation in sperm (Watanabe et al 2011.; Shang et al. 2019). The evolutionary conservation of *dpy-19* across species indicates its function is imperative to the developing nervous system, and our research here illuminates how disruptions to its function can lead to multiple impaired phenotypes.

INTRODUCTION

Neuronal migration. The process of cell migration in animals occurs in multiple contexts, including embryogenesis, the immune response, wound healing, angiogenesis, and cancer metastases (Kurosaka and Kashina 2008). During early development, cell migration is crucial for the proper morphology and physiology of an animal. Cells migrate in response to a complex system of signaling molecules, as well as being influenced by surrounding cells, the extracellular matrix, chemo-attractants, and mechanical constraints. The mechanisms responsible for cell migration are highly conserved in evolution, and defects in these mechanisms lead to severe malformations. In humans, early embryonic lethality, birth defects, congenital heart diseases, and physical and mental retardation can result from cell migration defects (Kurosaka and Kashina 2008). Abnormal neuron location due to improper migration during development affects brain connectivity and is

linked to multiple neurological disorders such as dyslexia, schizophrenia, and autism spectrum disorders (Pan, Wu, and Yuan 2019). The molecular pathways involved in the regulation of neuron migration are key to understanding these diseases and identifying targets for therapeutics.

In an effort to study the pathways and mechanisms underlying the localization of neurons, researchers have utilized model organisms to monitor the migration of cells. Rodents are the primary model used to study neuron migration, as its neuronal development is similar to most mammals. Rodent studies have identified the location and mechanisms of adult neurogenesis, as well as the migration patterns of new cells. Neuronal precursors can migrate either radially outward from the ventricular surface, or tangentially in the direction perpendicular to the radial axis. Projection neurons, which are usually excitatory, primarily undergo radial migration. Interneurons, which are typically inhibitory, migrate tangentially (Huilgol and Tole 2016). Neuron studies also utilize the zebrafish (*Danio rerio)* for its simple nervous system and ease of imaging. The transparent body of the zebrafish allows for *in vivo* screening of neurons and important proteins within neurons. Although zebrafish are more evolutionarily distant from humans than rodents, they are still useful for understanding neurobiology in context of human health. For example, potential therapeutic targets for MADD/glutaric aciduria type II, a genetic disease characterized by devastating neurological and metabolic symptoms, have been identified through studies using zebrafish (Song et al. 2009). *Caenorhabditis elegans* is also used frequently in research of the nervous system. Due to its transparent body, finite number of neurons, fully mapped and essentially invariable cellular lineage, and ability to easily mark cells with fluorescence, *C. elegans* provides an excellent model system to study the basics of developmental and cell biology (Corsi et al. 2015).

Over the course of several years, many genes involved in neuron migration in *C. elegans* have been identified. The genetics behind ventral-dorsal migration of neurons are well documented, including genes such as *slt-1, unc-5, unc-6, and unc-40,* which code for components of a pathway that mediates attractive signaling and guides neurons and/or axons to their final location (Hao et al.; Hedgecock et al. 2001). However, the genes and molecular pathways associated with anterior-posterior neuron migration is not completely understood. Researchers often look to the Q cell linage when studying the anterior-posterior neuron patterns, including polarization of initial migrations and intracellular signaling.

The Q cell lineage in *C. elegans*. The Q cell lineage begins in late embryogenesis when two Q neuroblasts – QL and QR – are produced. **Figure 1** provides a general summary of the divisions as well as the migration direction and final localization of Q cell lineage neurons. Their initial position lies between lateral seam cells V4 and V5, with QL on the left and QR on the right side of the embryo(Sulston and Horvitz 1977). Q cell migration begins shortly after the larva hatch, at which point QL polarizes and migrates a short distance towards the posterior over seam cell V5 along the anteroposterior axis. QR polarizes and migrates similarly, however it migrates over seam cell V4 towards the anterior. QL and QR undergo a series of cell divisions that are bilaterally symmetrical but migrate in opposite directions. The first division is symmetrical, generating two cells each (QR.a/p and QL.a/p, where the "a" and "p" refer to anterior and posterior daughter cells) which move in the same direction as their progenitor cells (**Figure 1**). QL.a migrates posteriorly between the V5 and V6 seam cells, where it asymmetrically divides, generating apoptotic cell QL.aa, and QL.ap, which develops into the oxygen sensory tail neuron, PQR (Middelkoop, Teije, Korswagen 2014). QL.p divides asymmetrically above seam cell V5 to produce a smaller apoptotic daughter cell, QL.pp, and a larger daughter cell, QL.pa, which divides symmetrically into QL.pap

and QL.paa. QL.paa differentiates into the mechanosensory PVM neuron while QL.pap differentiates into the SDQL interneuron (Sulston and Horvitz 1997).

QR.a migrates anteriorly from the seam cell V4 to V1, where it divides asymmetrically into an apoptotic cell, QR.aa, and a larger daughter, QR.ap. QR.ap migrates to the pharynx to differentiate into the oxygen sensory AQR neuron (Middelkoop, Teije, Korswagen 2014). QR.p migrates anteriorly and divides asymmetrically near seam cell V3 to produce a small daughter cell, QR.pp, that undergoes apoptosis. The larger daughter from this division, QR.pa, migrates further until it is between V2 and V1 seam cells where it symmetrically divides into QR.pap and QR.paa. QR.pap and QR.paa migrate bilaterally before differentiating into the SDQR interneuron and the AVM mechanosensory neurons, respectively. By the late L1 stage, descendants of the Q cell linage are dispersed from the pharynx to the anus (Sulston and Horvitz 1977). The bilateral to anteroposterior relationship of the Q cell lineage is unique and is one of the many reasons why researchers are curious about the mechanisms underlying the migrations.
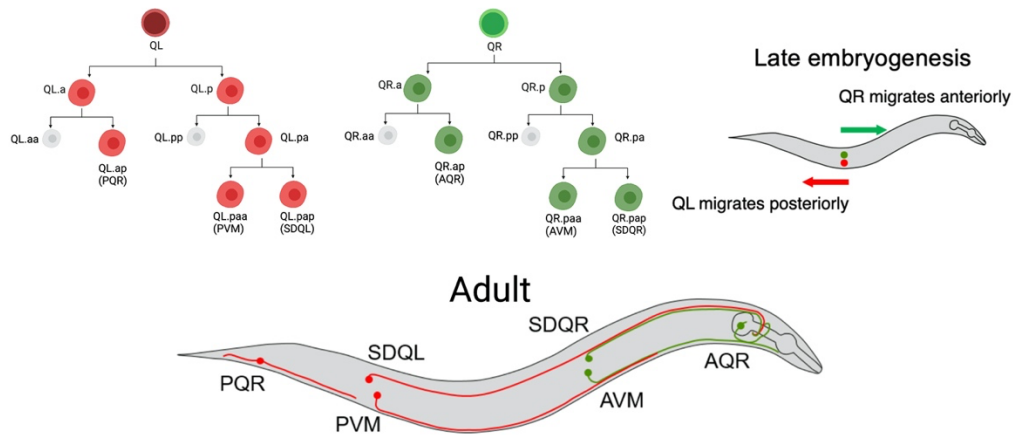
Figure 1. Q Cell Lineage and Migration. (Left) Schematic of the QL and QR lineage divisions, generating the P/AQR, P/AVM, and SDQL/R neurons. Gray cells indicate cells that undergo apoptosis. (Right) Initial polarization and migration of QL and QR along the anteroposterior body axis. (Bottom) Final positions of QR (green) and QL (red) descendants along with axon locations.

Regulation of Q Cell Migration. The migration of Q neuroblasts and their descendants occurs in two phases. First, the initial migration phase, when left-right asymmetry is established, the Q cells polarize and migrate a short distance. After the initial phase is the secondary migration phase, during which time there is maintenance of the left-right asymmetry and guidance of the Q neuroblast descendants to their final positions (Middelkoop, Teije, Korswagen 2014). While further research is needed to understand the full genetic regulation of Q cell neuroblast migration, it is known that EGL-20/Wnt signaling is utilized during the initial phase, as well as the netrin receptor UNC-40, and the transmembrane proteins MIG-21 and DPY-19. QL migrates posteriorly because of a difference in response threshold to EGL-20, causing canonical/ β-catenin Wnt/BAR-1 signaling and expression of *mab-5/Hox* to be activated only in QL (Whangbo and Kenyon 1999). MAB-5 is an essential protein containing a well-conserved homeobox motif, and any disruption in *mab-5* expression results in anterior migration of QL. UNC-40 is necessary for proper dorsoventral guidance of cells and axons, and mutations in *unc-40* cause randomized Q cell polarization (Honigberg and Kenyon 2000). Loss of *unc-40* causes the failure to express MAB-5 and/or causes the misexpression of MAB-5 in QR. *mig-21* encodes a thrombospondin repeat containing protein, that works in conjunction with UNC-40. Together they help to activate β-catenin Wnt signaling pathways that control the asymmetry by restricting posterior polarization to one of the two Q neuroblasts, as well as control the threshold of EGL-20 dependent interaction with QL and QR (Middelkoop et al. 2012). Mutations in *mig-21* produce defects similar to *unc-40* mutants, where QR and QL fail to polarize in one direction and repeatedly change direction during their initial migration. *dpy-19* encodes for a C-mannosyltransferase that modifies the thrombospondin repeats of MIG-21, producing the soluble form of MIG-21 that can be secreted.

DPY-19's role in neuroblast polarization and migration, as well as how it affects animal size is the focus of this thesis (Buettner et al. 2013).

Role of *dpy-19* in *C. elegans*. *dpy-19* was discovered in 1974 by Sydney Brenner, along with a series of other genes that when mutated resulted in "dumpy," or shorter than average worms. While the molecular role of *dpy-19* in regulating body length is not yet understood, the gene has been studied in connection to other roles. The gene encodes a transmembrane protein that contains 13 hydrophobic regions and shows homology with four human proteins, DPY19L1-4 (Middelkoop, Teije, Korswagen 2014). DPY19L1-3 are all known *C*-mannosyltransferases, while further research is needed to confirm if DPY19L4 functions similarly. DPY19L3 catalyzes the glycosylation of the RPE-spondin. The function of RPE-spondin remains unclear, however it is known to exist in the aorta extracellular matrix (Morishita et al. 2017). DPY19L1 is known to control radial migration of glutamatergic neurons, which suggests the gene has a conserved role in neuron migration (Watanabe et al. 2011). DPY19L2 functions in the development of the acrosome, a cap-like structure in the head of sperm cells. Its role is to anchor the developing acrosome to the nuclear membrane. A homozygous deletion of *DPY19L2* causes sperm with rounded heads without acrosomes, a condition called globozoospermia resulting in sterility (Shang et al. 2019).

While the molecular role of DPY-19 and its homologs as *C*-mannosyltransferases has been documented and some targets, such as RPE-spondin, UNC-5, and MIG-21, are known, it is likely that there are many other targets that DPY-19 modifies. Overall, little is known about this type of posttranslational modification. As of 2018, only 30 proteins had been identified as having *C*-mannosylation, all of which can be categorized as part of the thrombospondin type I repeat (TSR) and cytokine receptor type I families (Niwa and Simizu 2018). The characteristics of these families suggests that the modification regulates protein folding and secretion, and thereby affects the

functions of parental proteins. Although a rare modification, the importance of *C*-mannosylation is highlighted by the severity of the *dpy-19* mutant phenotypes on body size and neuroblast development (Buettner et al. 2013).

In *C. elegans*, mutations to *dpy-19* resemble *mig-21* and *unc-40* mutants, in that the QL and QR cells change direction sporadically during the initial migration(Honigberg and Kenyon 2000). Honigberg's 2000 study on the establishment of left/right asymmetry of the Q cell lineage revealed that *dpy-19* mutations *n1347n1348* and *mu78* result in some QL daughters migrating anteriorly, as well as some QR daughters migrating posteriorly. These results were not well quantified and were all done without benefit of the GFP markers, therefore utilization of fluorescently-labeled Q cells and their progeny, and presentation of quantified data would produce a more thorough study. The spontaneous mutation *dpy-19*(*cnj1*) that arose from the Killian Lab prompted further investigation into the role of *dpy-19* in proper migration of Q cell lineage descendants. However, *cnj1*, as well as other *dpy-19* mutations used in previous studies are not true or clean null alleles as they are either point mutations causing nonsense mutations, missense mutations, splicing defects, or they contain deletions of genes other than *dpy-19*. This thesis discusses the creation *dpy-19(cnj5),* a true null allele of *dpy-19* in effort to determine its effects on Q neuroblast migration, as well as its effects on animal length. The data shows that *dpy-19* is essential for proper posterior polarization and maintenance of migration direction of Q descendants and plays a role in maintaining proper animal length (Middelkoop et al. 2014).

MATERIALS AND METHODS

C. elegans **strains.** Strains were derived from the N2 (Bristol) strain, grown at 20°C and cultured using standard procedures described in Brenner (Brenner 1974). Mutant alleles *dpy-19(e1259)* and

dpy-19(e1314), as well as the LE3992 strain were obtained through the University of Minnesota's *Caenorhabditis* Genetics Center (CGC). The *dpy-19(cnj1)* mutant allele arose from a spontaneous mutation from the Killian Lab (Gus Parks, senior thesis in Molecular Biology 2020). *dpy-19(cnj5)* knockout allele was created using CRISPR microinjection and obtained through the Killian Lab (unpublished). Three transgenes were used for marking neurons in the Q lineage. *iaIs21[gcy-35p::GFP+unc-119(+)]* transgene acquired from CGC was used to mark the AQR, PQR, URXR/L, ALNL/R, BDUL/R, SDQL/R, AVM, and neurons in the tail (most likely PLNL/R) for control and *dpy-19* mutant Q cell lineage screening. AQR, PQR, AVM, PVM, PLM, and ALM neurons were marked with *zdIs5[mec-4::GFP + lin-15(+)]* for control and *dpy-19* mutant Q cell lineage screening (Clark and Chiu 2003). AQR and PQR neurons were marked with *wdIs51[PF49H12.4::GFP]* for control and *dpy-19* mutant Q cell lineage screening (Smith et al. 2010). While these fluorescent markers are expressed in some cells outside of the Q cell lineage, location and morphology were used to identify the appropriate cells.

Microscopy, imaging, and phenotypic analysis. For body length analyses, worms were picked at the late L4 or young adult life stage, placed on fresh NGM plates, and chilled on ice for approximately 5 minutes to slow down movement. Worms were imaged using a Leica M205 FA stereomicroscope at 130X and Leica LAS X software, then measured utilizing Leica's LAS X Analysis Segment Tool ($n = 30$ for each genotype). For neuron screening, animals were picked onto 2% agarose pad slides and immobilized using 0.25 mM levamisole. Animals were screened and imaged on Zeiss Axioskop microscope at 20X with ZEN/Zeiss imaging software by identifying the neurons present and their respective locations. $n = 50$ for all genotypes containing *wdIs51* and *zdIs5*. For *iaIs21* containing genotypes, $n = 50$ worms on their right sides and $n = 50$ worms on their left sides were used to get clear visuals of SDQRs and SDQLs, respectively.

Early Q cell Localization. *him-5(e1490)* males were crossed with *dpy-19(cnj5); iaIs21[gcy-35p::GFP+unc-119(+)]*. Male progeny were selected and crossed with hermaphrodites from the LE3992 strain, which contains the *Iqls80[SCMp::GFP::caax]* genotype encoding for GFP marker imbedded in the plasma membrane of Q cells to better visualize the cell migration direction. Self-progeny of this cross were screened for a non-roller, non-Cherry and *Iqls80[SCMp::GFP::caax*. Selected worms underwent self-fertilization to confirm all progeny were either homozygous for wildtype *dpy-19* and *Iqls80,* or homozygous for *dpy-19(cnj5)* and *Iqls80.*

Synchronization and screening of Q neuroblasts. M9 buffer was added to asynchronous NGM plates of the previously described strain and poured off to leave embryos. Newly hatched worms were picked every hour onto 2% agarose pad slides, immobilized using 0.25 mM levamisole, scored, and imaged on Zeiss Axioskop microscope at 100X with ZEN/Zeiss imaging software. *n* = 20 for control and *cnj5* genotypes.

RESULTS

Evaluation of the Dumpy phenotype in *dpy-19* mutants. While *dpy-19* is known to impact body size, the previously analyzed alleles were either non-null alleles or also impacted other neighboring genes. In order to determine the extent to which a true null allele of *dpy-19* affects the length of worms, various *dpy-19* mutations were screened, measured, and compared to age-matched wildtype L4 hermaphrodites. **Figure 2** illustrates the various *dpy-19* mutations utilized. *cnj1* arose spontaneously in 2019 in the Killian Lab and was confirmed to be a large deletion with a small insertion that deletes part of *dpy-19*, part of *pgl-2*, and completely deletes *F22B7.1* and *F22B7.14* (Gus Parks Senior thesis in Molecular Biology, 2020). The *e1259* allele causes a single amino acid change, and *e1314* is single nucleotide change at a splice acceptor (Honigberg and Kenyon 2000).

The true null allele of *dpy-19, cnj5,* which was created in the Killian Lab using CRISPR in 2020, deletes most of the *dpy-19* coding sequence while leaving neighboring and overlapping genes intact (unpublished). The L4 stage for control, *e1259, e1314, cnj5* and *cnj1* animals was determined by the presence of a developing vulva (**Figure 3A**). L4 control, *e1259, e1314, cnj5* and *cnj1* animals had average lengths of 763.6, 674.4, 468, 490.3, and 489.6 μm, respectively. The control animals had the largest amount of length variation (**Figure 3B**). An ANOVA analysis of the lengths showed that animals containing the wildtype allele of *dpy-19* were significantly different in length than the animals containing *cnj5, cnj1, e1314* and *e1259* alleles, with an adjusted p-value >0.0001. The *e1259* allele was also significantly different than all the mutant alleles in that the dumpy phenotype was less severe, with an adjusted value >0.0001 (Figure 3B). This less severe phenotype suggests that the single amino acid change (G to D) only partly disrupts *dpy-19* function in the regulation of body length.
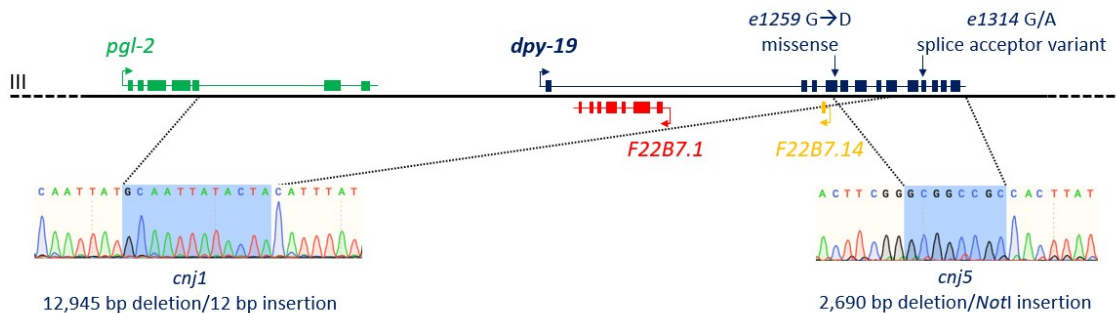

Figure 2. Graphical summary of the dpy-19 mutant alleles. The *cnj1* allele is a large deletion with a small insertion that deletes part of *dpy-19*, part of *pgl-2*, and completely deletes *F22B7.1* and *F22B7.14*. The *cnj5* allele deletes most of the *dpy-19* coding sequence while leaving neighboring and overlapping genes intact. *e1259* allele causes a single amino acid change, and *e1314* is single nucleotide change at a splice acceptor (Honigberg and Kenyon 2000).
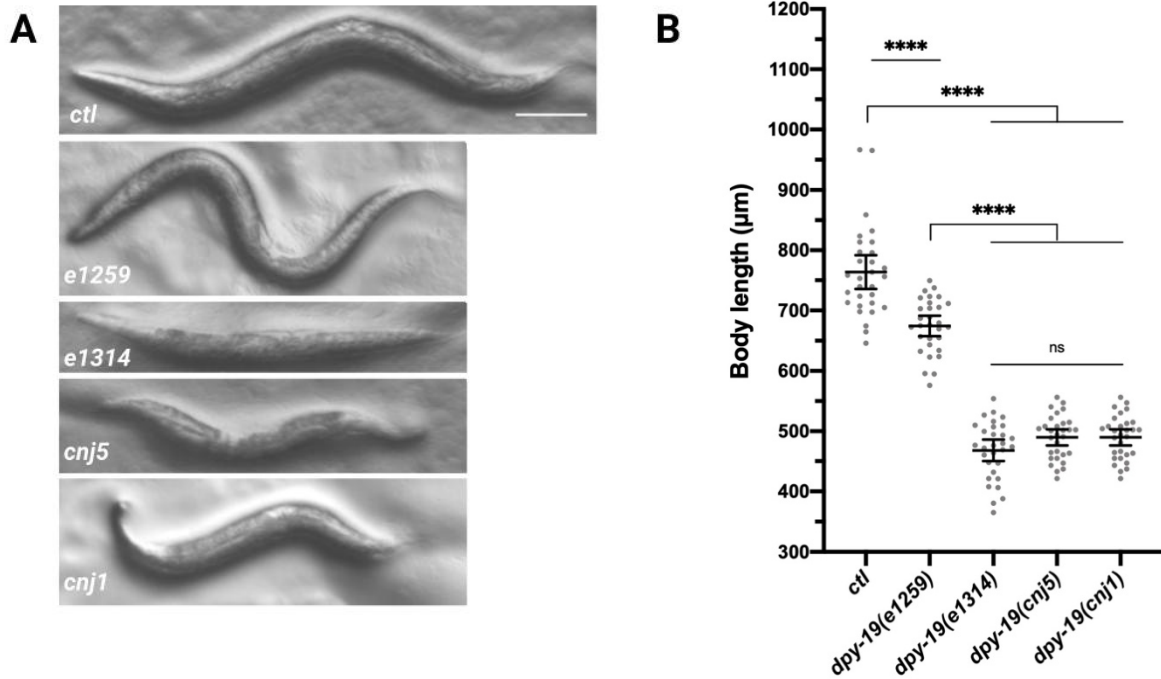
Figure 3. Dpy phenotype of various *dpy-19* mutants. (A) Control, *e1259, e1314, cnj5* and *cnj1* animals at the early-L4, with their heads aligned left. Bar = 100μm. (B) Scatter plot of body lengths from each genotype. Black bars indicate the mean and the 95% confidence interval. **** p<0.0001, ns = not significant.

Loss of *dpy-19* leads to Q lineage defects. Defects in *dpy-19* produced a range of phenotypic abnormalities, the most common being a lack of PQR, PVM and SDQL neurons in their expected locations, while displaying two bilateral AQR-like neurons in the head, two bilateral, dorsal AVM-like neurons, and two bilateral, ventral SDQR-like neurons, suggesting cells of the QL lineage migrated anteriorly and effectively duplicated their QR lineage counterparts (**Figure 4**). This phenotype will be referred to as Phenotype A, and the abnormally located neurons will be referred to as "converted" AQR, AVM, and SDQR, or cAQR, cAVM and cSDQR. Other phenotypes observed were similar in that there was a partial migration of the PQR, PVM and SDQL toward the anterior, but not to the same extent as Phenotype A (**Figure 5**). Neurons that appeared to be on the border of regions were classified as belonging to the more anterior region because even the slightest indication of abnormal location could be indicative of a defect in migration.

When scoring Q neuroblast descendants in control and *e1259, e1314, cnj5* and *cnj1* mutants using fluorescence microscopy, the AQR in all mutants was reliably positioned in region 1 with a small number of exceptions. *cnj1, cnj5* and *e1259* animals saw the AQR positioned in regions other than region 1 in 6%, 4% and 2% of animals, but did not produce a significantly different phenotype than the control (**Figure 5**). The AVM neuron was positioned in regions other than region 2 in 4% of *cnj1* mutants, 4% of *cnj5* 4% of *e1259* mutants. The control group revealed that SDQRs can have a localization range between the anterior region 3 and region 2, however all mutants except *e1259* animals produced a statistically different SDQR phenotype than the control, most notably the *e1314* mutant, which had the SDQR present in region 2 in 100% of the worms surveyed.
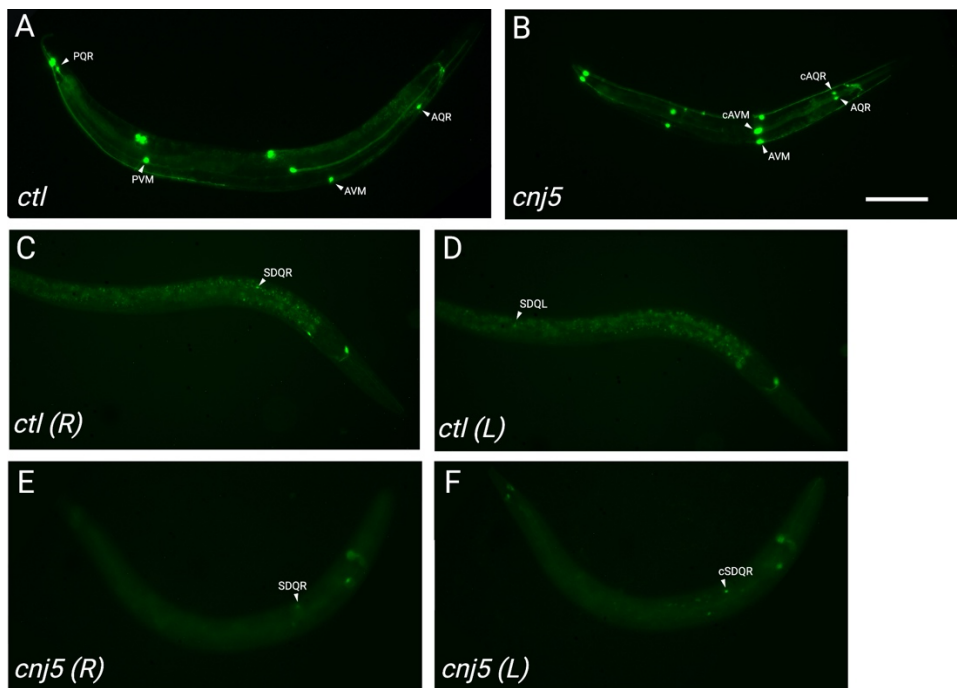

Figure 4. Q cell lineage defects results in Phenotype A. (A) Control animals expressing the *zdIs5* and *wdIs51* transgenes express GFP in 10 neurons including the Q neuroblast descendants AQR, PQR, AVM, and PVM. (B) *cnj5* mutants have an AQR, cAQR, an AVM and a cAVM, while also lacking the PQR and PVM. Bar = 100μm. (C) Control animals with GFP expressing in SDQR and (D) SDQL on the other side of the worm. (E) *cnj5* mutants have a typical SDQR location with a (F) cSDQR located on the opposite side of the worm, and no posterior SDQL

e1259 displayed the highest proportion of animals with abnormally located PQRs and PVMs. The PQR was abnormally located in 84% of *e1259* animals, with 70% of animals having a completely migrated to region 1 (**Figure 5**). *e1314, cnj5* and *cnj1* mutants presented with a PQR

in region 5 in 50%, 50% and 42% of animals, and presented with a cAQR in region 1 in 46%, 42% and 48% of animals, respectively. Pairwise comparisons between the control and each mutant revealed a statistical difference in PQR phenotype for every genotype pairing. Also, pairwise comparisons between *e1259* and all other mutants revealed a statistical difference in PQR phenotype for every genotype pairing. In 80% of *e1259* animals the PVM was missing from region 4 but presented with a cAVM in region 2. *e1314, cnj5* and *cnj1* mutants presented with a PVM in region 4 in 52%, 56% and 46% of animals, and presented with a cAVM in region 2 in 46%, 42% and 52% of animals, respectively. Pairwise comparisons between the control and each mutant revealed a statistical difference in PVM phenotype for every genotype pairing. In addition, pairwise comparisons between *e1259* and all other mutants revealed a statistical difference in PVM phenotype for every genotype pairing

SDQLs/cSDQRs in all mutants were more likely to have a partial incorrect phenotype, meaning they localized in region 3 between where a typical SDQL location and typical SDQR location, compared to the PQR and PVM. *e1314* mutants displayed the highest proportion of misplaced SDQLs, with 16% and 64% of animals presenting with cSDQRs in regions 3 or 2, respectively (**Figure 5**). Although percentages varied between genotype, the SDQL migrated anteriorly more than 50% of the time in all mutants. Pairwise comparisons between the control and each mutant revealed a statistical difference in SDQL phenotype for every genotype pairing. There were also significant differences in SDQL phenotypes between *e1259* and *e1314,* and *e1314* and *cnj5* (**Figure 5**).
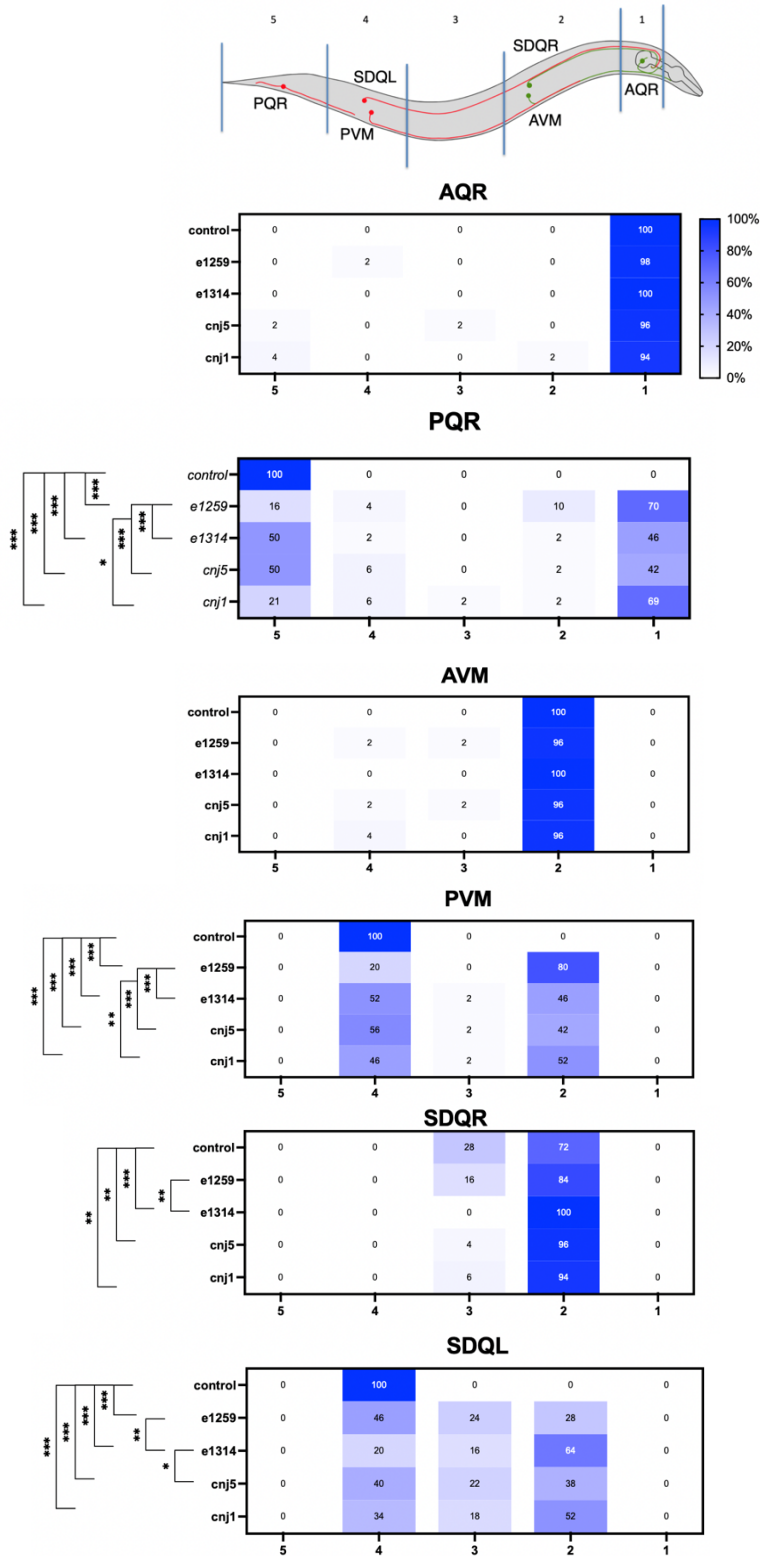
Figure 5. Regional variation of Q Lineage Neurons in Mutants. Heat map analysis depicting what percentage of animals had their AQR, PQR, AVM, PVM, SDQR and SDQL neurons located in each region (marked 1-5). Neurons that appeared to be on the border of regions were categorized as the more anterior region. Pairwise genotype combinations that displayed significant differences between are indicated with brackets. Non-significant pairwise genotype comparisons are unmarked. *** p<0.001, ** p ≤ 0.006, * p ≤ 0.030.

Q Cell pseudopods extend anteriorly in *cnj5*. To confirm the defects in PQR, PVM and SDQL location occur before the QR and QL cells differentiate, the QR and QL cells in L1 stage animals were marked with GFP (using *lqIs80*; see Materials and Methods) and screened for the direction of pseudopod growth. Pseudopods are cellular projections that are indicative of the direction of intended cellular migration. Only the QR and QL cells of controls and *cnj5* mutants were screened. The QR cells in control animals extended pseudopods anteriorly in 100% of animals, and the QL extended pseudopods posteriorly in 100% of animals (Table 1). QR cell migrated anteriorly in 97% of *cnj5* animals, while the QL migrated anteriorly in 56.57% of *cnj5* animals, and posteriorly in 43.44% of *cnj5* animals. Morphology of pseudopods varied between control and mutant animals, such that pseudopods of control QRs and QLs were elongated, and the pseudopods of *cnj5* QRs and QLs were shorter and spiky (**Figure 6A and B**). Although measurements were not taken of pseudopod length, a similar result was found in Honigberg and Kenyon (2000).
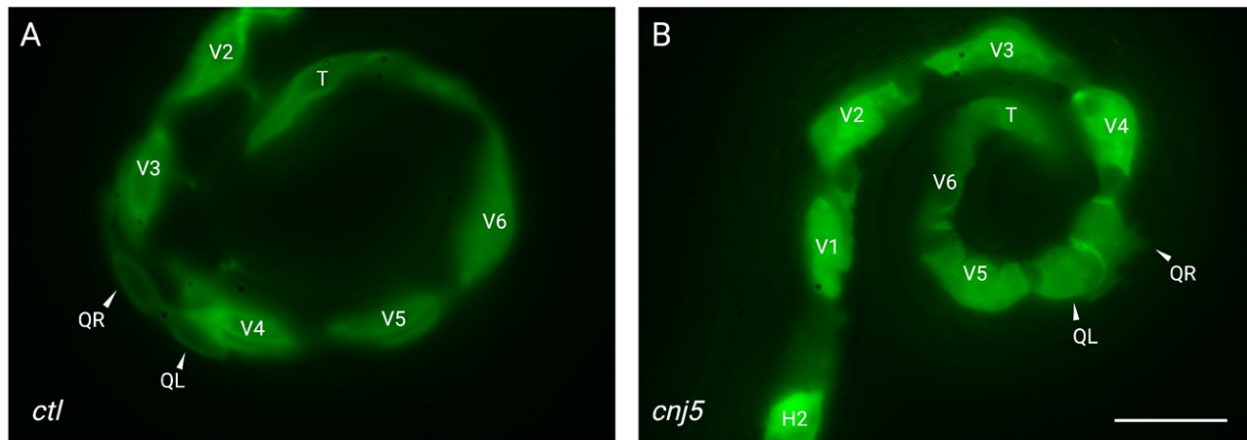
Figure 6. *cnj5* mutation results in QL cell pseudopods extending anteriorly. (A) Control animal with QR and QL cells fluorescing and their pseudopods projecting anteriorly and posteriorly, respectively, as well seam cells (v1-v5). (B) *cnj5* mutant QR and QL cell pseudopods projecting toward the head. Bar = 100 µm.

Genotype	% with QL pseudopods migrating anterior	% with QL pseudopods migrating posterior	% with QR pseudopods migrating anterior	% with QR pseudopods migrating posterior
+	0	100	100	0
cnj5	56.57	43.44	97	3

Table 1. Phenotypic scoring of the direction of QR and QL pseudopods in early L1 animals. *n=20*

DISCUSSION

This study reveals that the true null allele *dpy-19(cnj5)* significantly decreases the length of *C. elegans*, however the effects of the mutation are on par with other large scale deletion mutations like *cnj1* and the splicing defect mutation of *e1314*. This suggests that the missense mutation *e1259* results in a partial loss of function phenotype with respect to body length, where *e1259* mutants are shorter than controls but significantly longer than null mutants. Since *e1259* mutants are not a null allele for body length, it suggests it may be non-null for other phenotypes as well, such as neuron migration patterns. A topological analysis of the DPY19 homolog DPY19L3 reveals the importance of the C-terminal luminal region, suggesting it is required for proper *C*-mannosyltransferase activity. This provides a possible source of explanation for the effects of *e1314* mutants since the splicing error would lead to the disruption of the DPY19 C-terminal region (Niwa et al. 2018) It is also of note that the *dpy-19* mutants require more time to reach the L4 stage. Although the time required to reach L4 stage was not recorded for the mutants and further study is required to confirm a significant difference, this suggests proper *dpy-19* function is necessary for a normal growth time.

Upon analyzing how the various *dpy-19* mutants affect neuron migration, we see that the *e1259* mutants have the highest tendency for the PQR and PVM to be aberrantly located, while the *e1314* mutants have the highest tendency for the SDQL to be aberrantly located. This is surprising in two manners; firstly, the length analysis of the same mutants revealed that the mutants

containing larger deletions and disruptions (*cnj5, cnj1,* and *e1314)* have the most profound effects while *e1259* mutants result in a significantly less severe reduction in body size; secondly that the effects of a mutation vary between the PQR, PVM and SDQL neurons. For example, the location of PQR and PVM neurons in *e1259* animals are more likely to be affected than the location of the SDQL neuron. On the other hand, location of PQR and PVM neurons in *e1314* animals was less likely to be affected by the mutation than the location of the SDQL. Due to the inconsistency of effect intensity in each mutant, it is likely that the sensitivity to a loss or reduction of *dpy-19* in each specific neuron varies, possibly through a similar mechanism as the differences in response threshold to EGL-20 used during initial migration (Whangbo and Kenyon 1999). These specific neuron subtypes have not had their proteome fully analyzed and slight differences in cellular components between the PQR, PVM and SDQL could explain why their responses to a *dpy-19* mutation vary so greatly. It is also unknown if the cAQR, cAVM and cSDQR are fundamentally and mechanistically the same as their anterior counterparts, or if they retain the characteristics and function of PQR, PVM and SDQL neurons. Further studies would have to identify markers specific to the PQR, PVM and SDQL or neuron-specific activity assays to determine if the cAQR, cAVM and cSDQR are functionally equivalent the PQR, PVM and SDQL.

In 2000, Honigberg and Kenyon found that the molecular pathway including *unc-40*/DCC receptors and UNC-6/netrin ligands is needed for dorsal-ventral cell and axon migration in *C. elegans,* resulting in growth towards the ventral midline. In addition to this finding, they saw that *dpy-19* and *unc-40* mutants exhibited random initial polarization and migration of QR and QL cells. Here, we study the true null allele *dpy-19(cnj5)*, which we believe to be the first true null allele of the gene, since previous studies have utilized "null allele" *dpy-19(n1347n1348)* that deletes genes *F22B7.1* and *F22B7.14* on the opposite strand. Studies using *n1347n1348* found that

the QL projected anteriorly in 8% of animals, and QR projected incorrectly towards the posterior in 8% of animals. Our study of the direction of QR and QL pseudopod extension reveals that with a true *dpy-19* allele, the QL projects anteriorly in 56.57% of animals and QR projects posteriorly in 3% of animals. While this agrees with previous findings that *dpy-19* is needed for proper polarization of QR and QL, it reveals that a higher percentage of animals have a anterior migrating QL when *dpy-19* is null. These results show that QR and QL pseudopods extend anteriorly in the roughly the same proportion as cAQR, cAVM and cSDQR are found in the true *dpy-19* null allele *cnj5*, suggesting that the polarization of QR and QL must occur first, and differentiation occurs along the way. A possible further study could include a proper *dpy-19*-GFP fusion gene that would illuminate whether DPY-19 is present in the differentiated neurons or if it is only present in QR and QL cells at the beginning of migration. While Honigberg and Kenyon suggest that the *dpy-19* gene participates in prevention of "random" initial polarization of QL and QR, these results indicate *dpy-19* is also required for establishing the proper direction for migration of all QL descendants and the maintenance of the direction. The fluorescence microscopy images of *dpy-19* mutants show that the loss of *dpy-19* can cause all QL.x neurons to be aberrantly located in the region of QR.x final positions, but still on the left side of the body plan where the neurons would normally be located (**Figure 4**).

The distance cAQRs, cAVMs and cSDQRs must travel is a point of interest as well. Under normal conditions, the cell that generates the PQR travels roughly 19.3 ± 3.3 μm from its initial position above seam cell V4 and the cells destined to become the PVM and SDQL migrate a much shorter distance once located above seam cell V5 (Middelkoop, Teije, Korswagen 2014). While the distance migrated by the cAQR, cAVM and cSDQR were not measured, visually they are positioned in line with the AQR, AVM and SDQR, meaning the converted neurons must have

traveled roughly same distance as their anterior counterparts. The cell that eventually differentiates into AQR migrates 35.8 ± 6.8 μm from its initial position above seam cell V4, and cells that generate the AVM and SDQR migrate 16.7 ± 4.5 μm from the initial position. Clearly, the cells that become the cAQR, cAVM and cSDQR migrate a larger distance anteriorly than the cells destined to become the PQR, PVM and SDQL migrate posteriorly. Previous studies have suggested that *dpy-19* regulates the expression of *mab-5* in QL cells, which guides posterior migration, a function which becomes inhibited when *dpy-19* is impaired. When *mab-5* is inappropriately expressed in QR, it extends pseudopods posteriorly (Whangbo and Kenyon 1999). In this study, posterior migration of QR cells occurred at a low frequency, with what would be the AQR and AVM located in line with the PQR and PVM, respectively. This highlights a discrepancy in migrating distance effects. When *dpy-19* mutations manifest in a QR cell, it and descendants migrate a much shorter distance than when the QL and its descendants suffer from the same loss of function. From this, it appears that the role of *dpy-19* is not binary, or at least participates in a non-symmetrical system. This is in agreement with the current literature, which states DPY-19 acts as a *C*-mannosyltransferase on the thrombospondin repeats of MIG-21, creating soluble version of MIG-21 that controls a left-right asymmetric Wnt signaling responsible for the initial migration of QL/R (Buettner et al. 2013). This also provides an explanation as to why some animals containing null or null-like *dpy-19* alleles had normal cellular migration relative to controls. It is possible that some *dpy-19* mutants were able to use the insoluble form of MIG-21 to participate in the left-right asymmetric Wnt signaling, thus having proper migration of QL/R. DPY19 also modifies UNC-5, a netrin receptor involved in distal tip cell migration. This study cannot commit on how defects to *dpy-19* impact distal tip cell migration as only the cells of the Q lineage were visualized. However, it is known that defects to *unc-5* produce different Q lineage

phenotypes than *dpy-19* mutant, suggesting modification of UNC-5 is not a part of the Q lineage migration patterns (Honigberg and Kenyon 2000). While it is clear *dpy-19* has a role in determining direction of the Q cell linage migration, it is unknown the extent to which the pathways it participates in influences cell characteristics. More evidence is required to determine if on the molecular level the QR and QL descendants of *dpy-19* mutants are the same, however having these cells migrate similar distances suggests that the direction of migration influences cell motility and therefore possibly overall characteristics.

In conclusion, this research was able to confirm the role of dpy-19 in neuroblast polarization and migration using the true null allele *cnj5*. The discovery of the *e1259* and *e1314* mutants having a higher frequencies of abnormally located neurons when compared to more null and null-like alleles highlights how researchers must be selective when choosing mutations to include in neuron migration disorder models. When developing models, it is crucial that the alleles used are truly representative of the disease being studied. Hypothetically, incorporating *e1259* or *e1314* alleles into a disease model might overestimate the impact of defects to this gene. This research also highlights a possible sensitivity difference between neurons to dpy-19 levels, which can be seen when comparing PQR and PVM regional frequencies within a strain. As mentioned, future research into a full transciptome analysis of the AQR, AVM, SQDR and cAQR, cAVM and cSDQR of *dpy-19* mutants could provide insight into whether the converted species resemble their anterior counterparts in terms of gene expression. These cells migrate similar distances, suggesting that the direction of migration influences cell motility and therefore possibly overall characteristics.

ACKNOWLEDGEMENTS

REFERENCES

Brenner, S. "The Genetics of Caenorhabditis Elegans." *Genetics*, vol. 77, no. 1, 1974, https://doi.org/10.1093/genetics/77.1.71.

Buettner, Falk F. R., et al. "C. Elegans DPY-19 Is a C-Mannosyltransferase Glycosylating Thrombospondin Repeats." *Molecular Cell*, vol. 50, no. 2, 2013, https://doi.org/10.1016/j.molcel.2013.03.003.

Clark, Scott G., and Catherine Chiu. "C. Elegans ZAG-1, a Zn-Finger-Homeodomain Protein, Regulates Axonal Development and Neuronal Differentiation." *Development*, vol. 130, no. 16, 2003, https://doi.org/10.1242/dev.00571.

Corsi, Ann K., et al. "A Transparent Window into Biology: A Primer on Caenorhabditis Elegans." *WormBook : The Online Review of C. Elegans Biology*, 2015, pp. 1–31, https://doi.org/10.1895/wormbook.1.177.1.

Hao, Joe C., et al. "C. Elegans Slit Acts in Midline, Dorsal-Ventral, and Anterior-Posterior Guidance via the SAX-3/Robo Receptor." *Neuron*, vol. 32, no. 1, 2001, https://doi.org/10.1016/S0896-6273(01)00448-2.

Hedgecock, Edward M., et al. "The Unc-5, Unc-6, and Unc-40 Genes Guide Circumferential Migrations of Pioneer Axons and Mesodermal Cells on the Epidermis in C. Elegans." *Neuron*, vol. 4, no. 1, 1990, https://doi.org/10.1016/0896-6273(90)90444-K.

Honigberg, L., and C. Kenyon. "Establishment of Left/Right Asymmetry in Neuroblast Migration by UNC-40/DCC, UNC-73/Trio and DPY-19 Proteins in C. Elegans." *Development*, vol. 127, no. 21, 2000, https://doi.org/10.1242/dev.127.21.4655.

Huilgol, Dhananjay, and Shubha Tole. "Cell Migration in the Developing Rodent Olfactory System." *Cellular and Molecular Life Sciences*, vol. 73, no. 13, 2016, https://doi.org/10.1007/s00018-016-2172-7.

Kurosaka, Satoshi, and Anna Kashina. "Cell Biology of Embryonic Migration." *Birth Defects Research Part C - Embryo Today: Reviews*, vol. 84, no. 2, 2008, https://doi.org/10.1002/bdrc.20125.

Middelkoop, Teije C., et al. "The Thrombospondin Repeat Containing Protein MIG-21 Controls a Left-Right Asymmetric Wnt Signaling Response in Migrating C. Elegans Neuroblasts." *Developmental Biology*, vol. 361, no. 2, 2012, https://doi.org/10.1016/j.ydbio.2011.10.029.

Middelkoop, Teije C., and Hendrik C. Korswagen. "Development and Migration of the C. Elegans Q Neuroblasts and Their Descendants." *WormBook : The Online Review of C. Elegans Biology*, 2014, https://doi.org/10.1895/wormbook.1.173.1.

Morishita, Shohei, et al. "Dpy-19 like 3-Mediated C-Mannosylation and Expression Levels of RPE-Spondin in Human Tumor Cell Lines." *Oncology Letters*, vol. 14, no. 2, 2017, https://doi.org/10.3892/ol.2017.6465.

Niwa, Yuki, et al. "Topological Analysis of DPY19L3, a Human C-Mannosyltransferase." *FEBS Journal*, vol. 285, no. 6, 2018, https://doi.org/10.1111/febs.14398.

Niwa, Yuki, and Siro Simizu. "C-Mannosylation: Previous Studies and Future Research Perspectives." *Trends in Glycoscience and Glycotechnology*, vol. 30, no. 177, Gakushin Publishing Company, 1 Nov. 2018, pp. E231–38, https://doi.org/10.4052/tigg.1755.1E.

Pan, Yi Hsuan, et al. "Toward a Better Understanding of Neuronal Migration Deficits in Autism Spectrum Disorders." *Frontiers in Cell and Developmental Biology*, vol. 7, no. SEP, 2019, https://doi.org/10.3389/fcell.2019.00205.

Shang, Yong Liang, et al. "Novel DPY19L2 Variants in Globozoospermic Patients and the Overcoming This Male Infertility." *Asian Journal of Andrology*, vol. 21, no. 2, 2019, https://doi.org/10.4103/aja.aja_79_18.

Smith, Cody J., et al. "Time-Lapse Imaging and Cell-Specific Expression Profiling Reveal Dynamic Branching and Molecular Determinants of a Multi-Dendritic Nociceptor in C. Elegans." *Developmental Biology*, vol. 345, no. 1, 2010, https://doi.org/10.1016/j.ydbio.2010.05.502.

Song, Yuanquan, et al. "Mechanisms Underlying Metabolic and Neural Defects in Zebrafish and Human Multiple Acyl-CoA Dehydrogenase Deficiency (MADD)." *PLoS ONE*, vol. 4, no. 12, 2009, https://doi.org/10.1371/journal.pone.0008329.

Sulston, J. E., and H. R. Horvitz. "Post-Embryonic Cell Lineages of the Nematode, Caenorhabditis Elegans." *Developmental Biology*, vol. 56, no. 1, 1977, https://doi.org/10.1016/0012-1606(77)90158-0.

Watanabe, Keisuke, et al. "Dpy19l1, a Multi-Transmembrane Protein, Regulates the Radial Migration of Glutamatergic Neurons in the Developing Cerebral Cortex." *Development*, vol. 138, no. 22, 2011, https://doi.org/10.1242/dev.068155.

Whangbo, Jennifer, and Cynthia Kenyon. "A Wnt Signaling System That Specifies Two Patterns of Cell Migration in C. Elegans." *Molecular Cell*, vol. 4, no. 5, 1999, https://doi.org/10.1016/S1097-2765(00)80394-9.